

## Metastable chalcogen-related luminescent centers in silicon

A. Henry, E. Sörman, S. Andersson, W. M. Chen, B. Monemar, and E. Janzén

*Department of Physics and Measurement Technology, Linköping University, S-581 83 Linköping, Sweden*

(Received 20 August 1993)

Selenium-doped silicon quenched after heat treatment at 800 °C exhibits deep luminescence similar to that previously reported in sulfur-doped silicon. The corresponding Se-related complex gives rise to two deep bound-exciton (BE) photoluminescence (PL) emissions, which at low temperature have no-phonon (NP) lines at 955.5 meV ( $\text{Se}_A^0$ ) and 772.2 meV ( $\text{Se}_B^0$ ), respectively. A series of equidistant phonon replicas is observed with the same phonon energy as in the sulfur case. By increasing the temperature in the PL experiments associated BE excited-state lines are detected higher in energy with a separation of 10.5 and 12.4 meV, respectively, from the lowest NP lines. The metastability of both the S- and Se-related defects is investigated and discussed as well as the influence of the excitation photon energy on the intensity of the PL emission. The metastability is also confirmed by optically detected magnetic-resonance results, which also show that the ( $\text{S}_A^0$ ) and ( $\text{Se}_A^0$ ) lines correspond to an excited spin-triplet state. Both defects are found to have a low symmetry. When they are in the *A* configuration the symmetry is monoclinic *I* with one axis tilted approximately 20° from the  $[1\bar{1}1]$  axis in the (110) plane.

### I. INTRODUCTION

Impurities which introduce deep levels in a semiconductor band gap have attracted great interest for many years. Studies of chalcogen impurities in silicon have provided a broad base of experimental data of deep substitutional double donors as well as of more complex defects.<sup>1</sup> A sulfur-related defect, produced after a heating and quenching procedure, has attracted much attention, due partly to its high radiative efficiency.<sup>2</sup> Two characteristic photoluminescence (PL) emissions were attributed to the recombination of excitons bound at two sulfur-related isoelectronic systems  $S_A$  and  $S_B$ . These were investigated in more detail spectroscopically and shown in both cases to have a spin-triplet ground state with a singlet at about 9 meV higher in energy.<sup>3</sup> Later the two systems were shown to originate from two different configurations of the same metastable defect<sup>4–7</sup> which was proposed to be related to a sulfur pair defect and also involving copper.<sup>6</sup> Recently, similar highly efficient PL systems were reported for selenium-doped silicon.<sup>7,8</sup> However, very few spectroscopic details were presented so far for the Se case<sup>7</sup> and the metastability has not been proved.

The purpose of this work is to add more information on the spectroscopic properties and metastability behavior of the two chalcogen-related complexes, with particular emphasis on the new data for the Se-related defect. The PL and optically detected magnetic resonance (ODMR) techniques were used in this study as described in the following section. The experimental data obtained with both techniques are reported in Sec. III and are discussed in Sec. IV. The last section of this paper (Sec. IV) will summarize the most important results.

### II. EXPERIMENTAL PROCEDURE

#### A. Sample preparation

In this study we have used 0.4-mm-thick wafers cut from neutron-transmuted float-zone *n*-type Si from Top-sil Industry ( $\rho=100 \Omega \text{ cm}$ ). The diffusion at 1200 °C was performed in an evacuated quartz tube ( $10^{-6}$  Torr) where the samples were loaded together with Si and chalcogen powder. The diffusion time was 30 and 60 min for sulfur and selenium, respectively, which corresponds to diffusion depths of about 57 and 35  $\mu\text{m}$ , respectively.<sup>9–12</sup> The introduction of the chalcogen impurities into the silicon crystal was verified by measuring the change of resistivity. Finally to produce the radiative defect complexes studied in this work, the samples were heated at about 800 °C in a butane flame for 5–10 s and then thermally quenched by dropping in silicone oil.

#### B. Photoluminescence experiments

PL measurements were performed in the temperature range of 2–100 K. Preliminary measurements were made using the 514.5-nm line of an  $\text{Ar}^+$  ion laser as the excitation source. A neodymium-doped yttrium-aluminum-garnet (Nd:YAG) laser (1.06  $\mu\text{m}$ ) was used for high excitation power (around 50  $\text{mW}/\text{mm}^2$ ). For low excitation power (50  $\mu\text{W}/\text{mm}^2$ ) the light from a single monochromator was used, which enable the choice of excitation energy from 2 eV to below the silicon band gap (1.16 eV). The luminescence was dispersed either with a SPEX 1404 0.85-m double monochromator fitted with two 600 grooves/mm gratings blazed at 1.6  $\mu\text{m}$  (high spectral resolution) or a 0.6-m double monochromator Jobin

Yvon HDR (low spectral resolution). The latter monochromator system could record a spectrum in only 90 s. A liquid-nitrogen-cooled North Coast E0817 Ge detector was used with a mechanical chopper and a conventional lock-in technique to record the PL signal. The spectra were not corrected for the response of our detection system.

Using the 514.5-nm radiation from the Ar<sup>+</sup> laser the penetration depth of the excitation light is about 1  $\mu\text{m}$  at 2 K in Si material. However, the diffusion depth of the generated carriers is much larger and strongly dependent on the concentration of defects present in the crystal. This diffusion length can be on the order of a few tens of micrometers at 2 K. The Nd:YAG laser excitation allows the characterization of defects in the bulk of the sample.

### C. ODMR experiments

The ODMR experiments were performed with the aid of a modified Bruker ER-200D electron-spin resonance spectrometer, equipped with a TE<sub>011</sub> microwave cavity with optical access in all directions. The sample temperature could be varied from room temperature down to liquid He temperatures (4.2 K), where most of measurements were made, with an Oxford continuous-flow cryostat. The ODMR signal is in this case the change in luminescence caused by the amplitude modulated microwave field. A time-delayed technique (*D*-ODMR) had to be used to avoid the strong optically detected cyclotron resonance (OCDR) signal which otherwise obscures the quite weak ODMR signal. Details about the ODMR experimental procedure and setup were described previously.<sup>13</sup>

## III. EXPERIMENTAL RESULTS

### A. Photoluminescence spectra

Typical PL spectra recorded at two temperatures from a sulfur-doped silicon sample after the quenching procedure described above are shown in Fig. 1. At low temperature ( $T < 10$  K) and after laser excitation both systems show narrow no-phonon lines ( $S_A^0$  at 968.2 meV and

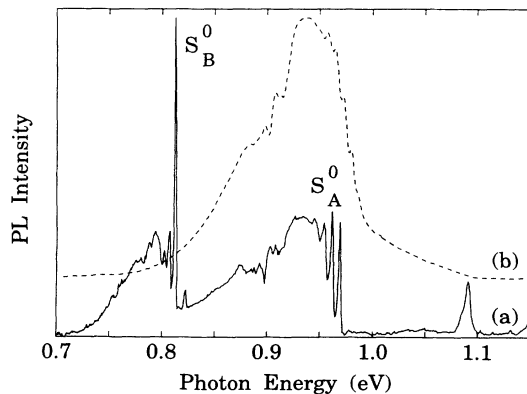


FIG. 1. PL spectra at 2 K (a) and 60 K (b) of sulfur-doped silicon after a heating and quenching procedure. The line structure at around 0.9 eV is due to water absorption.

$S_B^0$  at 812 meV, respectively) with various local-mode lines [Fig. 1(a)]. The positions of all observed lines are listed in Table I and as they agree with those previously reported by Beckett, Nissen, and Thewalt<sup>3</sup> their notation of the transitions was used. By increasing the measurement temperature ( $T > 10$  K) associated bound exciton (BE) excited state lines are detected higher in energy with a separation of 8.8 and 9.8 meV from the lower no-phonon (NP) lines, respectively. The two BE ground states,  $S_A^0$  and  $S_B^0$ , where shown to be spin triplets and the associated excited BE states were interpreted as the corresponding singlets.<sup>4</sup> At high temperatures ( $T > 50$  K) only the  $S_A$  emission is detected. As shown in Fig. 1(b) the  $S_A$  emission gives rise to a line structure between 980 and 950 meV and a broadband with a maximum intensity at about 930 meV due to phonon coupling to local modes. The total integrated PL intensity of the emission bands at high temperature [Fig. 1(b)] was found to be one order of magnitude higher than at low temperature [Fig. 1(a)].

Quenched selenium-doped silicon shows similar behavior as quenched sulfur-doped silicon. At high temperature ( $T > 60$  K) only the  $Se_A$  emission is detected whereas at low temperature and after laser excitation both the  $Se_A$  and  $Se_B$  PL systems can be observed. Figures 2(a) and 2(b) show PL spectra of the two systems at temperatures of 4 and 45 K, respectively. The total PL intensity at low temperature [Fig. 2(a)] is one order of magnitude lower than that recorded at higher temperature [Fig. 2(b)], and we must mention here that the total PL efficiency of the Se-doped samples was always weaker by about one order of magnitude than the S-doped samples. Together with the Se-related lines, other defects introduced by the heating and/or quenching procedure were often observed, such as copper lines (at about 1014 meV) and dislocation related lines (at 807 meV) [Fig. 2(a)]. High-resolution PL spectra of Se-doped silicon showing both systems separately, are displayed in Figs. 3

TABLE I. Isoelectronic bound-exciton no-phonon transitions observed by photoluminescence of sulfur- and selenium-related center.  $X$  denotes either S or Se. The energy positions associated to the S-related center are in agreement with the data obtained by Beckett, Nissen, and Thewalt (Ref. 3).

Line label	Energy position (meV)	
	S	Se
$X_A^0$	968.2	955.5
$^a X_A^0$		950.7
$^b X_A^0$	961.1	948.5
$^{2a} X_A^0$		945.9
$^{2b} X_A^0$	954	941.1
$^{-b} X_A^1$	982.4	972
$X_A^1$	977	966
$X_A^1$	969.9	958.6
$^{2b} X_A^1$	962	951.6
$^{3b} X_A^1$	954.7	944.4
$X_B^0$	812	772.2
$^b X_B^0$	805.3	765.7
$^{-b} X_B^1$	827.2	
$X_B^1$	821.9	784.6
$^b X_B^1$	815.2	777.7

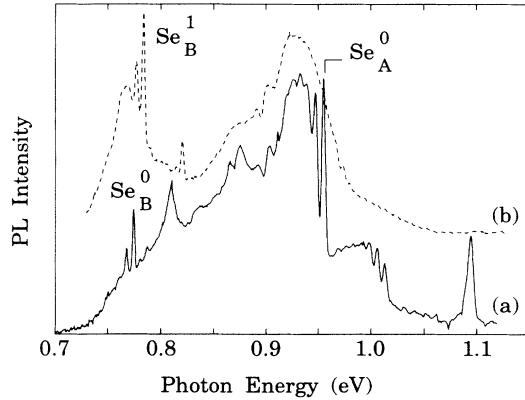


FIG. 2. PL spectra at 4 K (a) and 45 K (b) of selenium-doped silicon after a heating and quenching procedure. The notation of the lines is explained in the text.

and 4. The selenium-related transitions are labeled by analogy with the corresponding sulfur lines (see Table I). At low temperatures ( $T < 10$  K) both Se emissions show a narrow no-phonon (NP) line, at 955.5 meV [ $\text{Se}_A^0$  (Fig. 3)] and 772.2 meV [ $\text{Se}_B^0$  (Fig. 4)], respectively. Associated local-mode phonon lines separated with about 7.1 meV ( $\text{Se}_A^1$ ) and 6.7 meV ( $\text{Se}_B^1$ ), respectively, are also shown and they are successively broader and weaker (Figs. 3 and 4, respectively.) Optically detected magnetic resonance (ODMR) results which will be presented hereafter, show that the NP line  $\text{Se}_A^0$  corresponds to an excited spin-triplet state. The behavior is similar to the sulfur-related case and allows us to associate both the  $\text{Se}_A^0$  and  $\text{Se}_B^0$  lines with a spin-triplet initial states. By increasing the temperature of the experiment ( $T > 14$  K) the associated singlet lines are detected higher in energy with a separation of 10.5 and 12.4 meV from the triplets for  $\text{Se}_A^1$  and  $\text{Se}_B^1$ , respectively (see Figs. 3 and 4).

### B. Metastability

When the chalcogen-doped sample is cooled from high temperature ( $T > 60$  K) to low temperature (as, for example, 2 K) in darkness, only the *A* emission is seen. After

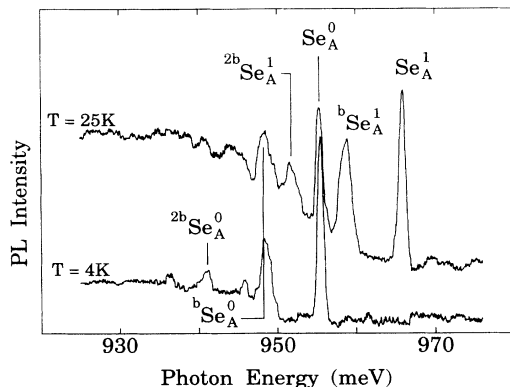


FIG. 3. High-resolution PL spectra of the  $\text{Se}_A$  emission at two different temperatures.

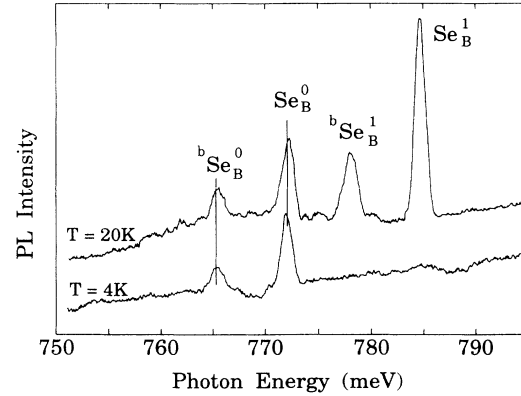


FIG. 4. High-resolution PL spectra of the  $\text{Se}_B$  emission at two different temperatures.

intense laser excitation at low temperature the *B* emission appears. This behavior shows the metastability of the chalcogen-related defect with a transformation from the *A* to the *B* configuration. As mentioned before, the PL efficiency of the Se system was found to be much lower than that of the S-related center. For this reason we will only show data from sulfur-doped samples although similar results could be obtained on Se-doped samples. The PL intensities of the  $\text{S}_A$  and  $\text{S}_B$  emissions as a function of excitation time  $t_e$  are depicted in Fig. 5. The decrease of the *A* emission intensity with increasing excitation time was found to be temperature independent [Fig. 5(a)]. However with the same experimental conditions the *B* emission reaches saturation when the time  $t_e$  increases whereas the *A* emission still decreases in intensity and the initial rate of the *B* emission intensity was observed to be slightly dependent on the temperature [Fig. 5(b)].

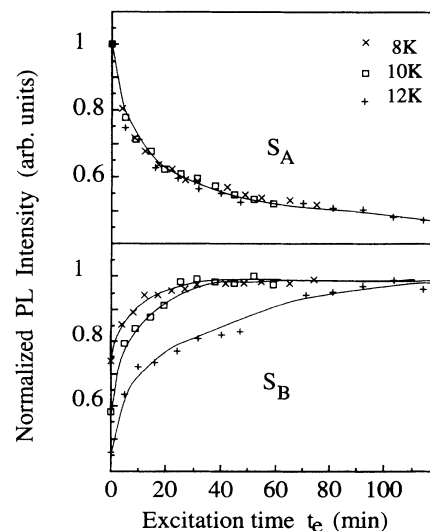


FIG. 5. PL intensity of the  $\text{S}_A$  and  $\text{S}_B$  emissions as a function of the excitation time  $t_e$ . The Nd:YAG laser was used as the excitation source and the excitation power was kept constant during all the experiments.

As mentioned above at high temperature ( $60 < T < 150$  K) only the *A* configuration is formed and gives rise to a PL spectrum described in Fig. 1(b). We show in Fig. 6 how the excitation photon energy influences this PL spectrum. For each spectrum the excitation energy is depicted by an arrow. All PL curves were normalized to the intensity of the excitation line. The integral PL intensity of the *A* emission is plotted as a function of the excitation photon energy in the inset of the figure. At high excitation photon energy, as with the Ar<sup>+</sup> ion laser, the PL intensity is maximum and it decreases when the photon energy of the excitation decreases. The *A* emission was detectable only with difficulty using an excitation energy close to the silicon band gap (1.17 eV) and not observed with excitation energy below 1.13 eV.

The transformation from the *A* to the *B* configuration at low temperature was also found to be dependent on the excitation photon energy. Figures 7(a) and 7(b) show the PL intensity of the *A* and *B* systems, respectively, as a function of the time  $t_e$  recorded at the temperature of 10 K using three different excitation photon energies (1.24, 1.21, and 1.19 eV). For this experiment the sample was cooled down from high temperature to 10 K in darkness. With high excitation photon energy ( $\geq 1.24$  eV) and after a short time the *B* emission shows its signature together with a decrease of the PL intensity of the *A* system [Fig. 7(a)]. However with a low excitation photon energy which was close to the silicon band gap, the transformation from the *A* to the *B* system is not observed even after 2 h of excitation.

### C. ODMR results

A conventional ODMR spectrum of the chalcogen-doped sample showed a predominant background signal due to a strong OADR signal, which obscured any possible detection of the ODMR signal from the S-related BE.

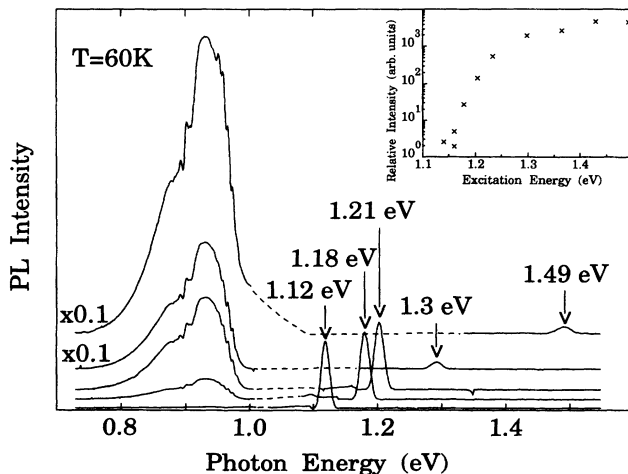


FIG. 6. PL spectra recorded at 60 K of a sulfur-doped silicon sample using the indicated excitation energies. All spectra are normalized to the intensity of the excitation line. The inset shows the total PL intensity as a function of the excitation energy.

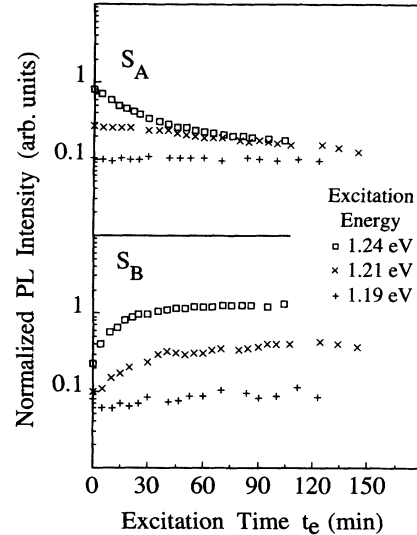


FIG. 7. PL intensity of the *A* and *B* configurations as a function of the exciton time  $t_e$  for three different excitation energies. The PL spectra were recorded at 10 K after a cooling in darkness of a sulfur-doped silicon sample.

However, the application of the *D*-ODMR technique was successful. In Figs. 8(a) and 8(b) we show two *D*-ODMR spectra when the detection wavelength is taken at around  $1.3 \mu\text{m}$  with the aid of optical band pass filter for the  $S_A$  and  $Se_A$  BE, respectively, and after cooling the samples in the dark. Because of the metastability of the defects the signal strength decreases in proportion to the time-integrated illumination intensity of the sample. To get the signal strength back a thermal annealing at temperatures exceeding 50 and 60 K for the case of S and Se, respectively, is required. The spectra are both identified to arise from a spin triplet, characterized by the lower-field  $\Delta M = \pm 2$  and the higher-field  $\Delta M = \pm 1$  microwave-induced electronic transitions. The complicated appearance of the  $\Delta M = \pm 1$  part is caused by the low symmetry

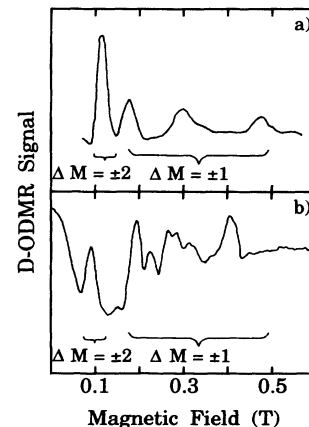


FIG. 8. *D*-ODMR spectra taken at 4 K from the (a)  $S_A$  BE triplet with the magnetic-field direction close to the [111] axis, and (b)  $Se_A$  BE triplet with the magnetic-field direction close to the [100] axis.

of the defect. The strange shape of the base line in the  $Se_A$  case [Fig. 8(b)] is caused by some remaining ODCR signal. A preliminary fit of the angular dependence of the ODMR signal with a spin Hamiltonian shows that the symmetry is monoclinic I in the both cases. In monoclinic I symmetry one of the spin axis is along the [110] direction (or equivalent directions), while the other two orthogonal axes can be rotated together in the (110) plane. Here it is experimentally found that the axes are rotated  $17^\circ$  and  $23^\circ$  for the  $S_A$  and  $Se_A$  BE, respectively, from the  $[1\bar{1}1]$  axis towards the  $[001]$  axis.<sup>14,15</sup>

The corresponding study for the  $B$  configuration in the sulfur case was done by cooling the sample in an intense  $Ar^+$  laser light and using a  $1.6\text{-}\mu\text{m}$  optical-band-pass filter. However, the  $D$ -ODMR signal from the  $S_B$  BE was one order of magnitude weaker than that from the  $S_A$  BE and contains only  $\Delta M = \pm 1$  resonance lines. A preliminary fit of the angular dependence of the  $D$ -ODMR signal with a spin Hamiltonian shows that the symmetry is triclinic. A detail study of the ODMR results will be presented elsewhere.<sup>14</sup>

Unfortunately it has so far not been possible to detect any ODMR signal from the  $Se_B$  state. However, by analogy with the sulphur case we believe that the symmetry of the Se-related defect in  $B$  configuration is also triclinic.

#### IV. DISCUSSION

The data presented above show that a metastable chalcogen-related complex is introduced in chalcogen-doped silicon after a heating and quenching procedure, for both the sulfur and selenium cases. The complexes give rise to isoelectronic bound-exciton spectra with sharp NP lines and local-mode satellites of similar energies. Four local modes were observed in the case of the sulfur complex,<sup>3</sup> whereas only two local modes are evident in our study for the selenium-related spectrum (Table II). They are the so-noted  $a$  phonon observed for the  $Se_A$  emission and the  $b$  phonon observed for the both  $Se_A$  and  $Se_B$  emission with an energy which corresponds exactly to that observed in the S-related spectra. The BE ground states detected at 968.2 and 812 meV in the sulfur case were shown to be spin triplets with the corresponding singlets at about 9 meV higher energies.<sup>4-6</sup> From the  $D$ -ODMR data and by comparison with the sulfur case we can say that the  $Se_A^0$  and  $Se_B^0$  no-phonon lines observed at low temperature arise from transitions from initial BE states, which are spin triplets, and with increasing temperature the corresponding singlet states are observed at 966 meV ( $Se_A^1$ ) and 784.6 meV ( $Se_B^1$ ), respectively.

TABLE II. Energies of the local-mode phonons observed in this luminescence study.

Phonon	Energy (meV)			
	$S_A$	$S_B$	$Se_A$	$Se_B$
$a$		5.4	4.6	
$b$	7.1	6.7	7.1	6.7

The energy separation between the triplet and singlet related PL lines for the chalcogen-related systems is then in the 10-meV range (8.8 and 9.8 meV for  $S_A$  and  $S_B$ , and 10.5 and 12.4 meV for  $Se_A$  and  $Se_B$ , respectively). This is not a common case in silicon where often only the singlet BE line is observed as, for example, for the carbon-related  $G$  and  $C$  lines.<sup>16</sup> However for a few complex defects the triplet-singlet splitting was observed, but only at a few meV ( $< 4$  meV).<sup>17-19</sup> Moreover, in the cases of Se and Te neutral double donors the triplet-singlet separations were found to be 6.1 and 8.6 meV, respectively.<sup>1</sup>

Low-energy phonon modes in the 10-meV range resonant with the acoustic-phonon continuum typically appear in several spectra associated with transition metals in silicon and especially the copper associated local mode energy was found to be 7.0 meV,<sup>16</sup> almost equal to the  $b$  phonon energy in the  $S_A$  and  $Se_A$  transitions. Moreover transition metals have very large diffusion coefficients at elevated temperatures and their associated PL spectra are often only observed after a fast thermal quenching procedure. The involvement of transition metals in the chalcogen centers is thus plausible and it has recently been shown that a copper atom is present in the sulfur-related defect.<sup>6</sup> Previously it was also shown that the both emissions  $S_A$  and  $S_B$  originated from two different configurations of the same defect.<sup>4,5</sup> We have suggested that the defect giving rise to these lines  $S_A$  and  $S_B$  were related to a defect containing a sulfur pair<sup>5</sup> since the energy separation between  $S_A^0$  and  $S_B^0$  ( $968.2 - 812 = 156.2$  meV) is nearly exactly the same as between the ground state  $1s(A_1^+)$  and the excited state  $1s(E^-)$  of the neutral sulfur pair ( $187.6 - 31.3 = 156.3$  meV).<sup>20</sup> Similar energetic comparisons can be done for the selenium case. The PL data show that the difference between the recombination energies  $Se_A^0$  and  $Se_B^0$  is  $955.5 - 772.2 = 183.3$  meV, whereas between the  $1s(A_1^+)$  and  $1s(E^-)$  states of the neutral selenium pair the separation is  $206.4 - 31.3 = 175.1$  meV,<sup>20</sup> i.e., only approximately similar. We suggest then that a chalcogen pair and a copper atom are involved in the defects giving rise to the PL systems described here. However this is in contradiction to a previous suggestion.<sup>21</sup>

The symmetry of the defects giving rise to the  $A$  configuration is found to be monoclinic I with one axis tilted approximately  $17^\circ$  and  $23^\circ$  for the S (Ref. 14) and Se (Ref. 15) defect, respectively, from the  $[1\bar{1}1]$  axis in the (110) plane. The small variation of the deviation could be influenced by the difference of atomic radii in the complex defect. The  $S_B$  configuration has a very weak  $D$ -ODMR signal which was distinctly different to the  $S_A$   $D$ -ODMR signal. This behavior shows that the  $S_A$  and  $S_B$  configurations have different symmetry, the  $B$  configuration is found to be triclinic.<sup>14</sup>

The metastability behavior is believed to be due to the motion of the copper atom in the complex defect. As the chalcogen-related defects have the same symmetry in the  $A$  configuration we suggest that the chalcogen pair involved in the defect does not play an important role for the metastability behavior, therefore being more as a "spectator." The copper atom is thus directly involved in the optical transitions observed, with probably the exci-

ton hole localized on a bond to the copper atom, since the zero-field ODMR data show that the Cu atom has a different local environment for the two configurations.<sup>22</sup>

From the study of the influence of the excitation photon energy on the PL spectrum (Fig. 6) we conclude that for the observation of the *A* system an excitation with high photon energy, higher than the silicon band gap, is needed. This behavior indicates that free carriers are needed to observe the *A* configuration. The observation of the  $S_A$  related lines reported by Beckett, Nissen, and Thewalt<sup>3</sup> when the 1.32- $\mu\text{m}$  line of a Nd:YAG laser was used as excitation source was interpreted as due to two-step process. Similarly, the very slow configuration conversion with the 1.32- $\mu\text{m}$  photoexcitation reported by Singh<sup>7</sup> we believe is due to the creation of free carriers via a two-step process. The conversion rate from the stable to the metastable configuration is independent of temperature (Fig. 5) but strongly dependent of the excitation photon energy (Fig. 7), e.g., on the concentration of free excitons created by the excitation. This is agreement with the excitonic Auger model for the mechanism of the configurational change of the metastable defects in silicon.<sup>23</sup>

## V. SUMMARY

Similar to the case of thermally quenched sulfur-doped silicon, a metastable selenium-related complex defect is reported to give rise to two deep characteristic photoluminescence (PL) spectra. At low temperature the deep bound-exciton (BE) PL emissions have no-phonon (NP) lines at 955.5 meV ( $\text{Se}_A^0$ ) and 772.2 meV ( $\text{Se}_B^0$ ), respectively, and a series of equidistant phonon replicas is observed with the same energy as in the sulfur case. At somewhat increased temperatures associated BE excited state lines are detected higher in energy with a separation of 10.5 and 12.4 meV, respectively, from the lowest NP lines. A metastable behavior is observed in the PL experiments for both the S- and Se-related defects and the data show that free carriers are needed for the configurational change of the defects. The metastability is confirmed by optically detected magnetic resonance results, which also show that the BE lines correspond to a transition from a spin-triplet state. The defects are found to have a monoclinic *I* symmetry with one spin axis tilted approximately 20° from the  $[1\bar{1}1]$  axis in the (110) plane when they are in the *A* configuration, and a triclinic symmetry is expected for the *B* configuration.

<sup>1</sup>H. G. Grimmeiss and E. Janzén, in *Deep Centers in Semiconductors*, 2nd ed., edited by S. T. Pantelides (Gordon and Breach, New York, 1992), p. 87, and references therein.

<sup>2</sup>T. G. Brown, and D. G. Hall, *Appl. Phys. Lett.* **49**, 245 (1986).

<sup>3</sup>D. S. J. Beckett, M. K. Nissen, and M. L. W. Thewalt, *Phys. Rev. B* **40**, 9618 (1989).

<sup>4</sup>M. Singh, E. C. Lightowers, G. Davies, C. Jeynes, and K. J. Reeson, *Mater. Sci. Eng. B* **4**, 303 (1989).

<sup>5</sup>A. Henry, W. M. Chen, E. Janzén, and B. Monemar, in *Proceedings of the 20th International Conference on the Physics of Semiconductors*, edited by E. M. Anastassakis and J. D. Joannopoulos (World Scientific, Singapore, 1990), p. 545.

<sup>6</sup>W. M. Chen, M. Singh, A. Henry, E. Janzén, B. Monemar, A. M. Frens, M. T. Bennebroek, J. Schmidt, K. J. Reeson, and R. M. Gwilliam, *Mater. Sci. Forum* **83-87**, 251 (1992).

<sup>7</sup>M. Singh, Ph.D. thesis, King's College, 1992.

<sup>8</sup>P. L. Bradfield, T. G. Brown, and D. G. Hall, *Phys. Rev. B* **38**, 3533 (1988).

<sup>9</sup>P. L. Gruzin, S. V. Zemski, A. D. Bulkin, and N. M. Marakarov, *Fiz. Tekh. Poluprovodn.* **7**, 835 (1973) [*Sov. Phys. Semicond.* **7**, 1241 (1974)].

<sup>10</sup>R. O. Carlson, R. N. Hall, and E. M. Pell, *J. Phys. Chem. Solids* **8**, 81 (1957).

<sup>11</sup>C. S. Kim, and M. Sakata, *Jpn. J. Appl. Phys.* **18**, 247 (1979).

<sup>12</sup>H. G. Grimmeiss, E. Janzén, B. Skarstam, and A. Lodding, *J. Appl. Phys.* **51**, 6238 (1980).

<sup>13</sup>W. M. Chen and B. Monemar, *J. Appl. Phys.* **68**, 2506 (1990).

<sup>14</sup>W. M. Chen, M. Singh, B. Monemar, A. Henry, E. Janzén, A. M. Frens, M. T. Bennebroek, and J. Schmidt (unpublished).

<sup>15</sup>E. Sörman *et al.* (unpublished).

<sup>16</sup>G. Davies, *Rep. Phys.* **176**, 83 (1989), and references therein.

<sup>17</sup>S. P. Watkins, M. L. W. Thewalt, and T. Steiner, *Phys. Rev. B* **29**, 5727 (1984).

<sup>18</sup>E. C. Lightowers, L. T. Canham, G. Davies, M. L. W. Thewalt, and S. P. Watkins, *Phys. Rev. B* **29**, 4517 (1984).

<sup>19</sup>H. D. Mohring, J. Weber, and R. Sauer, *Phys. Rev. B* **30**, 894 (1984).

<sup>20</sup>E. Janzén, R. Stedman, G. Grossmann, and H. G. Grimmeiss, *Phys. Rev. B* **29**, 1907 (1984).

<sup>21</sup>T. G. Brown, P. L. Bradfield, and D. G. Hall, *Appl. Phys. Lett.* **51**, 1585 (1987).

<sup>22</sup>A. M. Frens, M. T. Bennebroek, J. Schmidt, W. M. Chen, and B. Monemar, *Phys. Rev. B* **46**, 12 316 (1992).

<sup>23</sup>W. M. Chen, J. H. Svensson, E. Janzén, B. Monemar, A. Henry, A. M. Frens, M. T. Bennebroek, and J. Schmidt, *Phys. Rev. Lett.* **71**, 416 (1993).